Turkish Journal of Electrical Engineering & Computer Sciences

http://journals.tubitak.gov.tr/elektrik/

Research Article

Turk J Elec Eng & Comp Sci
(2016) 24: 1265 – 1278

doi:10.3906/elk-1312-140

A novel approach of design and analysis of fractal antenna using a neurocomputational method for reconfigurable RF MEMS antenna

Paras CHAWLA*, Rajesh KHANNA
Electronics & Communication Engineering Department, Chandigarh Engineering College, Chandigarh Group of Colleges, Landran, Greater Mohali, Punjab, India

Received: 20.12 .2013 • **Accepted/Published Online:** 26.02.2014 • **Final Version:** 23.03.2016

Abstract: A mathematical neural approach/artificial neural network (ANN) for the design of a swastika-shaped reconfigurable antenna as a feedforward side is proposed. Further design parameter calculations using the reverse procedure of the above method is presented. Neural network computational is one of the optimization methods that could be considered to improve the performance of the device. In this paper, the proposed planar antenna up to the 2nd iteration is simulated using finite element method-based HFSS software. The developed ANN algorithm method allows the optimization of the antenna to be carried out by exchanging repetitive simulations and also provides reduced processing times while still retaining great accuracy as compared to traditional mathematical formulation. The simulated S-parameter (return loss) results of the proposed antenna are verified with the ANN and show good agreement. Furthermore, for proof of concept, the above proposed antenna as well as a swastika-shaped reconfigurable antenna (2nd iteration) with radio frequency microelectromechanical system switches are fabricated and tested using a vector network analyzer. The results presented here show that the antenna works well in the frequency range of 1.5 to 6.5 GHz and resonates on multiple bands. The novelty of the approach described here offers ease of designing the process using the ANN algorithm, maintaining the miniaturization of antenna size, multiband behavior, and utility of the antenna in the mobile terminal.

Key words: Antenna design, modeling and measurements, radiofrequency switch, artificial neural network, reconfigurable antennas and components, applications and standards (mobile and wireless), fractal antenna

1. Introduction

In the present age of electronic and communication handheld devices, the prime requirement of a wireless communication system is that a single antenna must be useful for a number of applications that are working on different frequency bands by merely changing their physical dimensions. Another matter of concern is that the wireless communication systems are also moving towards miniaturization very rapidly [1]. All these requirements of today's wireless communication systems have led antenna researchers to work on the various aspects of antenna design with distinctive ideas of manufacturing and synthesis. To fulfill the modern requirements of wireless systems, several efforts have been made, and it has been concluded by antenna researchers that the naturally occurring fractal geometries can also be used as useful antenna elements that facilitate the present scenario of communication systems with the ease of flexibility in resonances and features like low profile and small size [1,2].

In recent years, one can list and observe the development of a number of antennas that are based on

*Correspondence: paras.chawla@thapar.edu

different fractal geometries. Some of these fractal designs have been particularly deployed in miniaturization of the antenna elements, while other fractal geometries serve the multiband characteristics for the antennas [1,2].

The Sierpinski gasket, better known as a Sierpinski triangle, was the first fractal shape preferred for antenna design purposes [3]. In recent years, antenna researchers have tried other fractal shapes, too, including the Sierpinski carpet, Hilbert curve, hexagonal shape [4], cactus shape, and Giuseppe Peano. All these fractal geometries are intended to design low-profile and multiresonant antennas with considerable gain, often with similar radiation characteristics in their bands.

In this article, the concept of fractals has been applied to the geometry of a square patch planar antenna to obtain multiband frequency operation. Here the new type of self-similar shape selected for design of the patch is a swastika shape, which is shown in Figure 1. Artificial neural networks (ANNs) are among the popular smart techniques in solving engineering and mathematical problems. An ANN consists of neurons that are organized into different layers. These neurons are simple and many, contain nonlinear types of functional blocks, and are mutually connected by very similar synaptic weights. During the learning process, these synaptic weights could be weakened or strengthened and therefore help the data to be kept in the ANN [5,6]. The benefits, feasibility, and flexibility of ANNs have no formula necessary to design a planar antenna due to the empirical nature, based on the observation of physical phenomena, less computational time as compared with other optimization methods, and compatibility with commercial electromagnetics software [5–8]. Neural networks can be used for the applications of wireless communications. In the area of microwave applications, a neural network has been used to design rectangular planar antennae. Similarly, an ANN was used for the design of circular antennae [7], calculating different parameters such as resonant frequency and input impedance of circular microstrip antenna. Here, an ANN has been used for the design of a swastika-shaped fractal antenna. Figure 1 shows the process of iteration for the swastika fractal antenna up to the 2nd iteration.

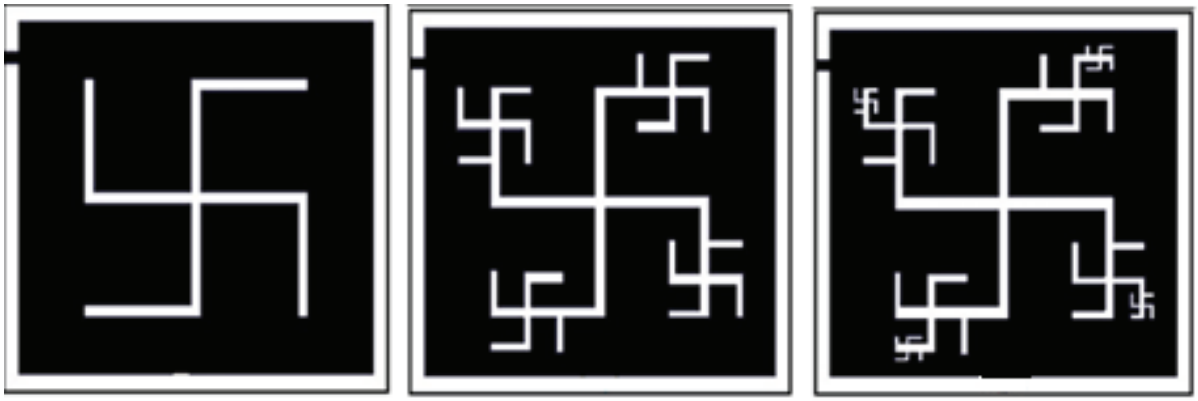

Figure 1. Swastika slot fractal antenna up to 2nd iteration.

In Section 7, the above proposed 2nd iteration planar swastika antenna is converted into a reconfigurable antenna (RA) by introducing radio frequency microelectromechanical system (RF MEMS) switches. The RF MEMS switch has been preferred in this work over FET and PIN diode switches because of high isolation, low insertion loss, and low power supply consumption [9,10]. The reconfigurable antenna [11,12] designed in this manner is helpful to achieve more multiband frequencies.

2. Design of swastika planar antenna

Design of planar antennae includes the definite data of the dielectric constant (ε_r), the resonant frequency, and thickness of the substrate (t). Initially, for designing the swastika fractal antenna, the following dimensions and materials were considered: area of slot (A), 1575 mm^3 (30 mm $\times$ 35 mm $\times$ 1.5 mm); Roger RO4350 material having thickness of 0.762 mm; and dielectric constant 3.48 to get zero iteration geometry as depicted in Figure 1. Then the antenna was simulated using HFSS software. Return losses versus frequency plot are shown in Figure 2. From the figure, it is clear that the return loss was less than –10 dB at three frequencies of 2.32 GHz, 2.58 GHz, and 6.43 GHz. Therefore, for design of this antenna, the aforementioned three resonant frequencies, thickness of substrate, and dielectric constant are taken as input; number of iterations, i.e. I = 0, and area of slot equal to 1575 mm^3 are taken as output. For this iteration, thus, the input G_1, G_2, G_3, G_4, G_5, t, ε_r = 2.32, 2.58, 0, 0, 6.43, 0.762, 3.48 and output A, I = 1575, 0 have been taken. Then the dimensions of length, breadth, and width of slots are equal to one-third of the 0th iteration dimensions, i.e. 10.05 mm $\times$ 11.15 mm $\times$ 1 mm has dropped from this structure to get the 1st iteration geometry depicted in Figure 1. The structure was simulated again and a graph of return loss versus frequency was plotted, as shown in Figure 3. From this plot, it is clear that return losses are less than –10 dB at four frequencies of 2.1 GHz, 2.98 GHz, 4.08 GHz, and 6.02 GHz. For the design of the first stage of this antenna, the aforementioned four resonant frequencies, thickness of substrate, and dielectric constant are taken as input, and number of iterations, i.e. I = 1, and area of slot equal to 112.07 mm^3 are taken as output. Therefore, the inputs G_1, G_2, G_3, G_4, G_5, t, ε_r = 2.1, 2.98, 0, 4.08, 6.02, 0.762, 3.48 and output A, I = 112.07,1 have been considered for the ANN.

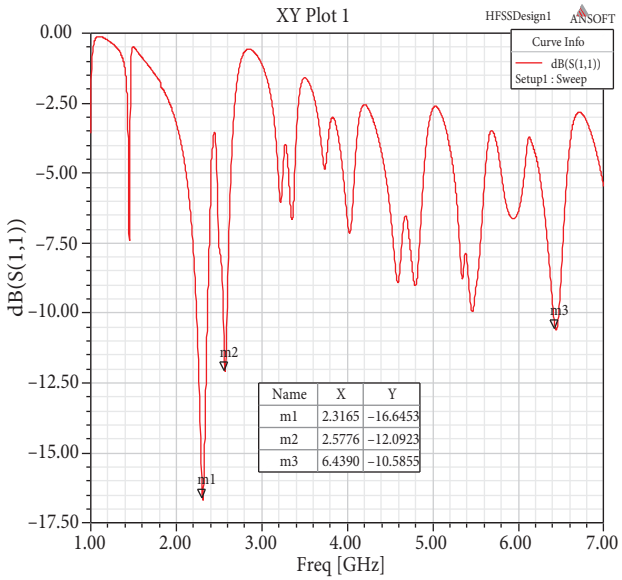

Figure 2. Return loss versus frequency plot of fractal antenna for 0th iteration.

Afterwards, the dimensions of the slot are dropped 1/9th times the dimensions of the 0th iteration, i.e. 112.07 from 1st iteration geometry, to get 2nd iteration geometry, which is shown in Figure 1. This geometry has again been simulated using HFSS software and a graph was plotted between return losses versus frequency as depicted in Figure 4. From this figure, it is clear that return losses are less than –10 dB at the five frequencies of 2.14 GHz, 2.86 GHz, 3.93 GHz, 4.14 GHz, and 6.28 GHz, respectively. For designing this iteration the aforementioned five resonant frequencies, thickness of substrate, and dielectric constant have been taken as

input, and number of iterations, i.e. I = 2, and area of slot equal to 8.369 mm^3 have been taken as output. Therefore, for this iteration the input G_1, G_2, G_3, G_4, G_5, t, ε_r = 2.14, 2.86, 3.93, 4.14, 5.89, 0.762, 3.48 and the output A, I = 8.369, 2 have been considered for the ANN.

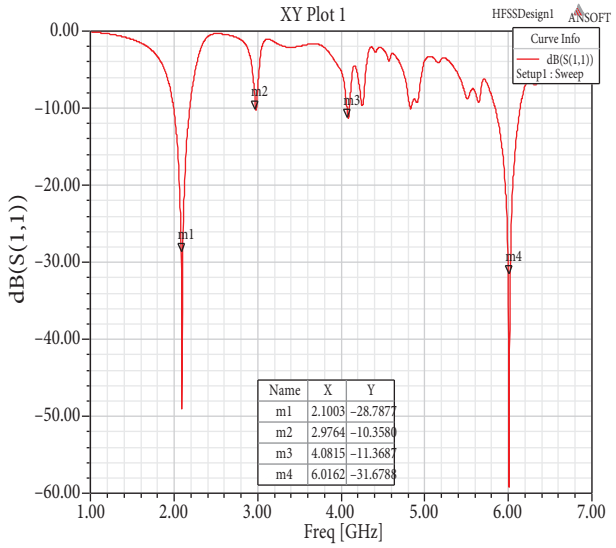

Figure 3. Return loss versus frequency plot of fractal antenna for 1st iteration.

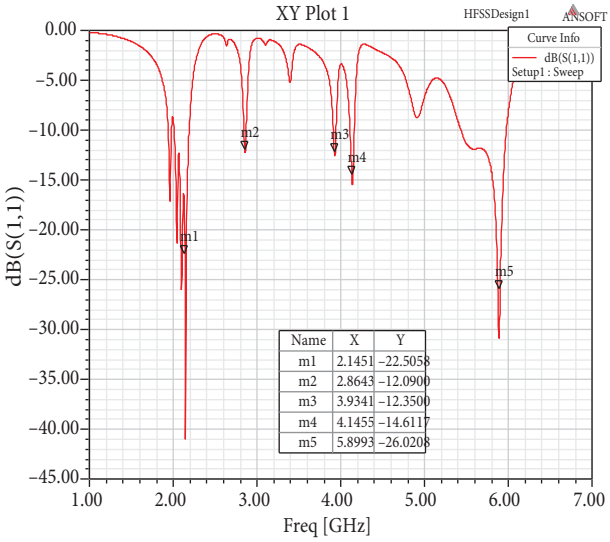

Figure 4. Return loss versus frequency plot of fractal antenna for 2nd iteration.

In this way, a set of 75 input-output pairs are generated for training and a set of 25 pairs are generated for validation of neural network.

3. Neurocomputational modeling for design of swastika fractal antenna

The neurocomputational model for design of a swastika fractal antenna is as shown in Figure 5, indicating that the proposed FFBP-ANN model has six inputs (resonant frequencies G_1 to G_5, thickness of substrate 't', dielectric constant of substrate 'ε_r', number of iterations 'I', and area of antenna (A), and two outputs. Neural networks trained on data dictionary have been applied to calculate the area of the swastika fractal antenna, i.e. 'A', and number of iterations 'I' for given values of resonant frequencies 'G', thickness of substrate 't', and dielectric constant of substrate 'ε_r'. The proposed ANN model contains tan sigmoidal neurons in the form of

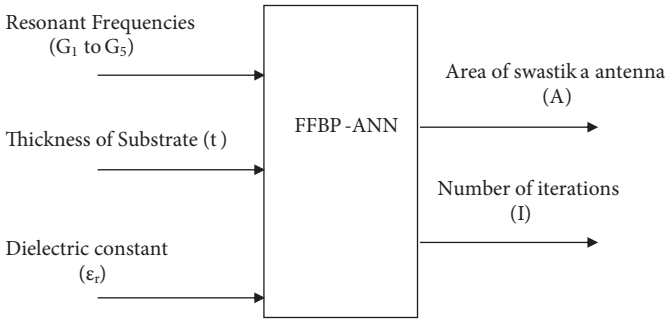

Figure 5. Neurocomputational model for design of swastika fractal antenna.

one hidden layer having activation function equal to 'f_1'. The input information is given to the first level and that output is set as input data for the final output level. The intermediate hidden level output is transmitted in the form of neurons to the final output level, which contains two neurons, and as a final point it calculates the network output. In this case, the activation function is considered as 'f_2'.

Output of the proposed ANN is computed by the following.

$$X = f_2([OW](f_1([FW][Y] + [FB]) + [OB]) \tag{1}$$

$$Y = \begin{bmatrix} G_1 \\ G_2 \\ G_3 \\ G_4 \\ G_5 \\ t_i \\ ?r_i \end{bmatrix} \tag{2}$$

$$_X = \begin{bmatrix} A_i \\ I_i \end{bmatrix} \tag{3}$$

$$FW = \begin{bmatrix} fw_{1,1} & \cdots & fw_{1,7} \\ \vdots & \ddots & \vdots \\ fw_{35,1} & \cdots & fw_{35,7} \end{bmatrix} \tag{4}$$

$$_{FW} = \begin{bmatrix} fb_1 \\ \vdots \\ \vdots \\ \vdots \\ fb_{15} \end{bmatrix} \tag{5}$$

$$OB = \begin{bmatrix} ob_1 \\ ob_2 \end{bmatrix} \tag{6}$$

$$[OB] = \begin{bmatrix} ow_{11} & ow_{12} & \cdots & ow_{1,35} \\ ow_{21} & ow_{22} & \cdots & ow_{2,35} \end{bmatrix} \tag{7}$$

The MSE, i.e. the performance index, is given by the following.

$$MSE = \frac{1}{n} \sum\nolimits_{i=1}^{n} [y_i - F_{ANN}(x_i)]^2 \tag{8}$$

The proposed model, trained with the Levenberg–Marquardt algorithm and with structure 7-35-2 as depicted in Figure 6, is found as the best-fit structure for estimation of dimensions of the swastika fractal antenna. This ANN structure has an input layer with seven input neurons. A hidden layer has 35 hidden neurons and an output layer has two output neurons.

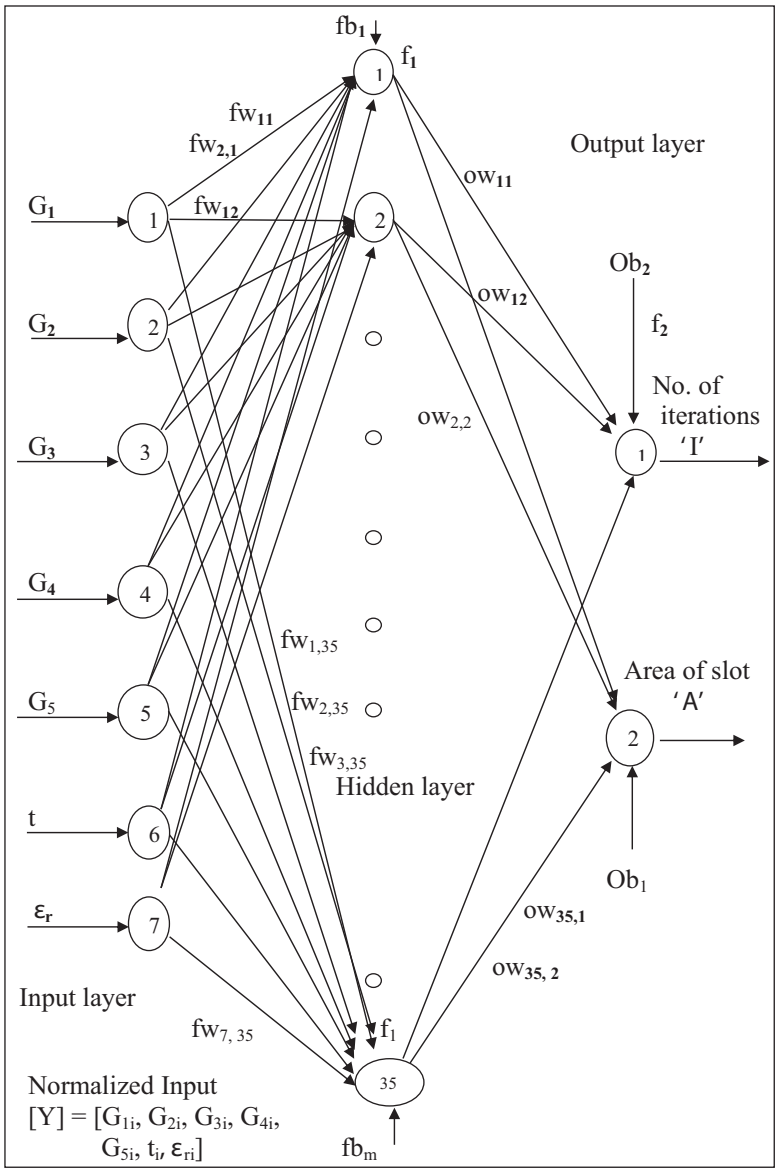

Figure 6. Proposed FFBP-ANN-based neurocomputational model for design of swastika fractal antenna.

4. Neurocomputational modeling for analysis of swastika fractal antenna

For analysis of the swastika fractal antenna, a reverse process is done. Thickness of substrate (t), dielectric constant (ε_r), area of swastika fractal antenna (A), and number of iterations (I) are taken as input. Resonant frequencies G_1 to G_5 are taken as output. The neurocomputational model for the analysis of the swastika fractal planar antenna is shown in Figure 7. In the above example for analysis of the swastika fractal antenna

for zero iterations, we took input A, t, ε_r, I = 1575, 0.762, 3.48, 0 and G_1, G_2, G_3, G_4, G_5 = 2.32, 2.58, 0, 0, 6.43 as output. For the first iteration, we took input A, t, ε_r, I= 112.07, 0.762, 3.48, 1 and G_1, G_2, G_3, G_4, G_5 = 2.1, 2.98, 0, 4.08, 6.02 as output. For the 2nd iteration, we took input A, t, ε_r, I = 8.369, 0.762, 3.48, 2 and G_1, G_2, G_3, G_4, G_5 = 2.14, 2.86, 3.93, 4.14, 5.89 as output.

For analysis of the swastika fractal antenna, the proposed model trained with the Levenberg–Marquardt algorithm and with structure 4-35-5 as shown in Figure 8 is found to be the best-fit structure. ANNs trained on statistics dictionaries have been useful to estimate the resonant frequencies of swastika fractal antennae, i.e. G_1 to G_5, for a given value of area 'A' and number of iterations 'I', thickness of substrate 't', and dielectric constant of substrate 'ε_r'. Furthermore, the implemented neural model had a similar model to that followed for training purposes.

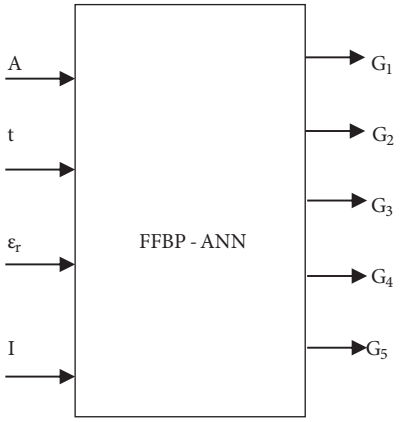

Figure 7. Neurocomputational model for calculating the resonant frequency of the swastika fractal antenna.

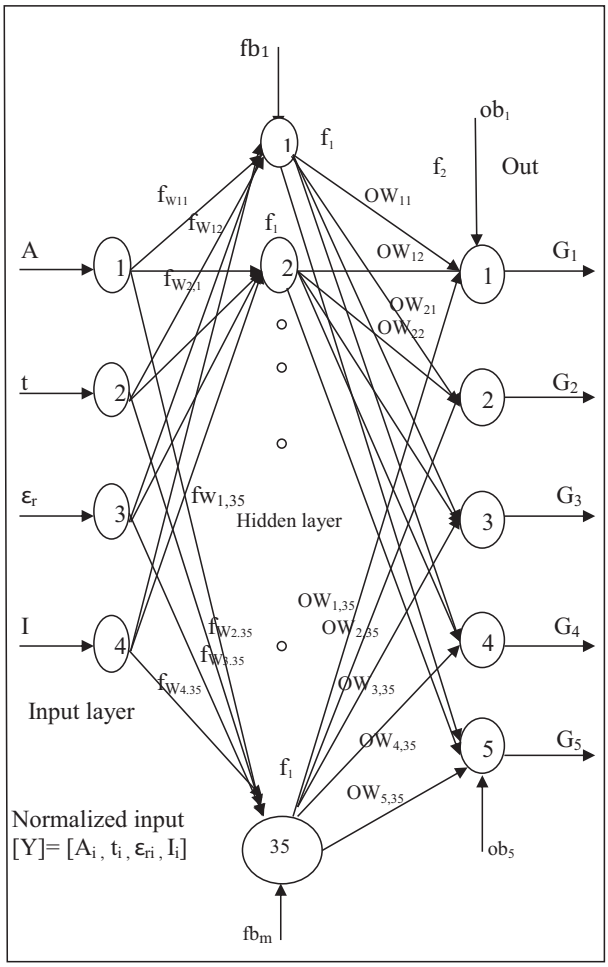

Figure 8. Proposed FFBP-ANN-based neurocomputational model for estimating resonant frequency of the swastika fractal antenna.

The first layer with four neurons receives input data and its output is given as input to the hidden layer with 35 neurons. The output from the neurons of the hidden layer is transmitted to the output layer of five neurons, which finally computes the network output. Output of the proposed ANN is computed by the

following.

$$X = f_2([OW](f_1([FW][Y] + [FB]) + [OB]) \tag{9}$$

$$Y = \begin{bmatrix} A_i \\ t_i \\ \varepsilon r_i \\ I_i \end{bmatrix} \tag{10}$$

$$X = \begin{bmatrix} G_1 \\ G_2 \\ G_3 \\ G_4 \\ G_5 \end{bmatrix} \tag{11}$$

$$FW = \begin{bmatrix} fw_{1,1} & \cdots & fw_{1,4} \\ \vdots & \ddots & \vdots \\ fw_{35,1} & \cdots & fw_{35,4} \end{bmatrix} \tag{12}$$

$$[FB] = \begin{bmatrix} fb_1 \\ \vdots \\ \vdots \\ \vdots \\ fb_{35} \end{bmatrix} \tag{13}$$

$$[OB] = \begin{bmatrix} ob_1 \\ ob_2 \\ ob_3 \\ ob_4 \\ ob_5 \end{bmatrix} \tag{14}$$

$$[OW] = \begin{bmatrix} ow_{1,1} & \cdots & ow_{1,35} \\ \vdots & \ddots & \vdots \\ ow_{5,1} & \cdots & ow_{5,35} \end{bmatrix} \tag{15}$$

5. Results of the trained ANN

In order to calculate the performance of the proposed FFBP-ANN-based model for the swastika fractal antenna design and analysis, results of simulation were obtained using HFSS software for correct determination of dimensions of this antenna. The ANN was trained with 75 input–output training patterns. The training data obtained above were used for training the proposed 7-35-2 ANN structure for design and 4-35-5 for analysis of the swastika fractal antenna. Results in terms of performance parameters such as number of epochs taken for training, performance goal mean square error (MSE), maximum absolute error, and percentage error for design and analysis are shown in Tables 1 and 2. It has been detected that a total number of 292 epochs is desired to decrease the MSE level to a small value of 9.89e-007 for design and 380 epochs are desired to decrease the MSE level to a small value of 9.87e-006 for analysis of the swastika fractal antenna. Achievement of such a low value of the performance goal (MSE) indicates that the trained ANN model is an accurate model for design and analysis of the swastika fractal antenna. The absolute error value and percentage error at each value of area and number of iteration for design and resonant frequencies for analysis as a result of the training study with the Levenberg–Marquardt algorithm are shown in Tables 1 and 2, respectively. The maximum errors for estimating the area and number of iterations were 0.0074 and 7.19e-004, respectively. Furthermore, percentage error for estimating the area and number of iterations of the swastika antenna were 0.39 and 0.035, respectively. The small value of this error indicates that the neural model is an exact model for the design. Similarly, the maximum errors for estimating the resonant frequencies of the antenna were 0.011, 0.007, 0.027, 0.005, and 0.004, respectively.

Table 1. Results of the FFBP-ANN-based model for the estimation of area and stage number of swastika fractal antenna for training data.

Training algorithm	Number of neurons in hidden layer	Epochs	MSE	Absolute error for estimation of		% error for estimation of	
				Area 'A'	Iteration number 'I'	Area 'A'	Iteration number 'I'
Levenberg–Marquardt algorithm	35	292	9.89e-007	0.0074	7.19e-004	0.39	0.035

Table 2. Results of FFBP-ANN-based model for the estimation of resonant frequencies of swastika fractal antenna for training data.

Training algorithm	Number of neurons in hidden layer	Epochs	MSE	Absolute error for estimation of					% error for estimation of				
				G_1	G_2	G_3	G_4	G_5	G_1	G_2	G_3	G_4	G_5
Levenberg–Marquardt algorithm	35	380	9.87e -007	0.011	0.007	0.027	0.005	0.004	0.18	0.083	0.471	0.472	0.034

6. Results of validity study

In order to test the results for the swastika fractal antenna design we generated 45 input–output patterns for testing the proposed trained 7-35-2 ANN structure for design and 4-35-5 ANN structure for study of this antenna. The absolute error and error (percentage FS) at each value of area, number of iteration for design,

and resonant frequency for analysis of this antenna as a result of validation study are shown in Tables 3 and 4, respectively. Attainment of such small values of these errors (absolute and percentage FS) further indicates that the neural network is a perfect model for the fractal antenna design and analysis.

Table 3. Comparison of error obtained for finding the area and stage number of swastika fractal antenna using FFBP-ANN 6-35-2 structure for validation of data.

	Absolute error for estimation of		% error for estimation of	
Parameters	Area 'A'	Iteration number 'I'	Area 'A'	Iteration number 'I'
	0.060	0.032	2.899	1.601

Table 4. Comparison of error obtained for finding the resonant frequencies of fractalantenna using FFBP-ANN 4-35-5 structure for validation of data.

	Absolute error for estimation of					% error for estimation of				
Parameters	G_1	G_2	G_3	G_4	G_5	G_1	G_2	G_3	G_4	G_5
	0.017	0.035	0.123	0.089	0.068	0.291	1.200	0.386	2.211	2.171

7. Reconfigurable antenna designing and testing setup

In this section the above proposed 2nd iteration planar swastika antenna was converted into a reconfigurable antenna by introducing RF MEMS switches. The location of switches, the schematics, and the dimensions (in mm) of the proposed reconfigurable antenna are shown in Figure 9. Initially, the minimum gap of RF switch size was provided between each individual swastika-shaped slot. According to the geometry of the antenna, a total of eight switching elements were placed, as shown in Figure 9. The simulation of the antenna with RF switches was done with HFSS software. There were a total of $2^8 = 256$ switching configurations positions (i.e. off and on) of eight switches, and accordingly the antenna was operated and therefore reconfigured at different frequencies. The s-parameter results show that RA worked well for the 1.5–6.5 GHz frequency band.

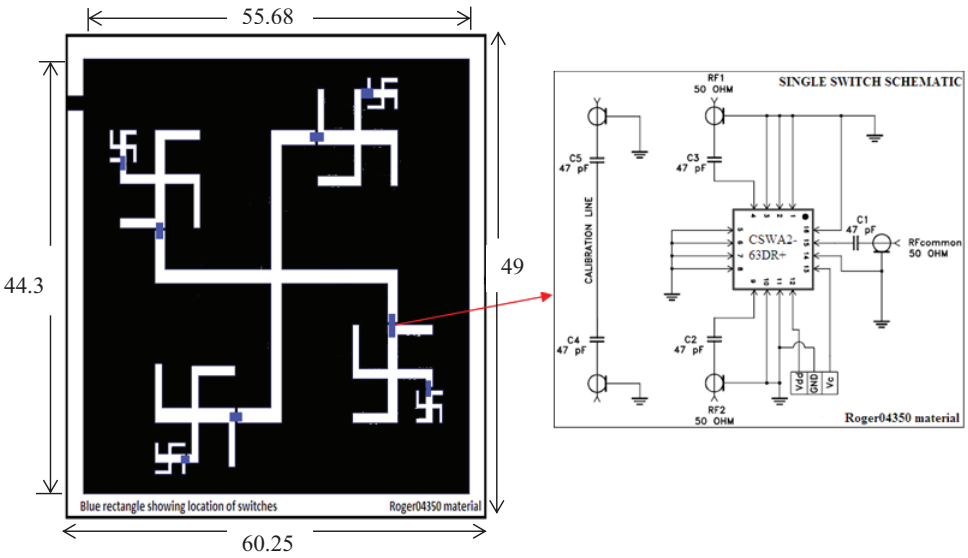

Figure 9. Reconfigurable swastika-antenna dimensions and RF switch schematic.

The normalized radiation pattern performances plotted for the RA at extreme switching configuration (all-on and all-off) are included next. At given solution frequency, the variation of current distribution on the surface of the RA with different switching configurations is the reason for the difference in the patterns. Simulated normalized relative power patterns, i.e. YZ-, XZ- and XY-cut patterns, are shown in Figures 10a–10d at solution frequency of 4 GHz. The combined magnitude of the electric field components in the desired polarization are shown next in Figures 10e and 10f. A figure-eight pattern in the XY-plane as shown in Figure 10b signifies a dipole type of radiation pattern. The RA, as expected, achieves fairly normalized omnidirectional patterns. From the 3D radiation pattern plot (not shown here), it was observed that the antenna behaves directionally in the elevation plane and nondirectionally in the azimuth plane. Furthermore, the RA showed well-behaved linearly polarized characteristics as the axial ratio (E_y/E_x) was more than one at theta equal to zero.

The proposed RF switches' reconfigurable antenna fabrication and electromagnetic measurement setup are majorly divided into five subdivisions, the swastika planar antenna, SPDT RF switches (CSWA2-63DR+) printed circuit board (PCB) including DC biasing pad and tracks, variable DC regulated power supply to change the desired configuration (on/off) of RF switches, Agilent Technologies E5071C vector network analyzer (VNA), and the anechoic chamber. For simulation purposes, the resistive MEMS RF switch selected for the swastika antenna was taken from the authors' own previous work [11], which showed very good electromagnetic properties. Its equivalent absorptive ceramic SPDT RF switch having similar isolation, insertion loss, and matching equal to 50 ohm, was considered for proof of concept. The aforementioned RF switch consumes much less power (in μW) and the supply current value is around 18 μA. It is a hermetic package, small in size (4 mm $\times$ 4 mm $\times$ 1.2 mm), with a low profile and an internal driver circuit.

Furthermore, the wide bandwidth lies from 0.5 to 6.5 GHz, which made this switch suitable for the proposed reconfigurable antenna design. A separate sheet of Roger RO4350 material having the same thickness and dielectric constant as that of the planar swastika antenna was used for integration of RF switches. To block the DC components, highly stable on-chip capacitor dielectrics C0G (NP0) ceramics of 47 pF was used. The regulated power supply varies from 1.28 to 4.89 V and was designed to operate RF switches. The RF common, RF1, and RF2 pads (as shown in Figures 9 and 11) from integrated switches were directly connected to the swastika antenna through excellent quality thin copper wires having thickness of 0.025 mm. The complete setup of testing the reconfigurable antenna with switches is shown in Figure 11. The S-parameter comparison results are shown in Table 5.

8. Conclusion

In this paper, ANN-based computation is proposed for developing a high performance system to reduce the development cycle that otherwise requires lengthy procedures and design cycles by conventional methods. The swastika fractal antenna described here used a feedforward backpropagation artificial neural network (FFBP-ANN) with a hidden layer as an approximate model for design and analysis. The results of the proposed methods are quite promising. From the results, it has been observed that the proposed modeling technique is very convenient to model the ANN for predicting the design parameters under specified conditions and applications of neural networks. By the given modeling techniques, the design of the antenna seems to be a simple, inexpensive, and correct method. The results obtained by the discussed methods compared very well with simulated results.

Furthermore, the 2nd iteration planar swastika antenna was converted into a reconfigurable antenna by applying RF MEMS switches. The new novel reconfigurable swastika-shaped multiband antenna with RF

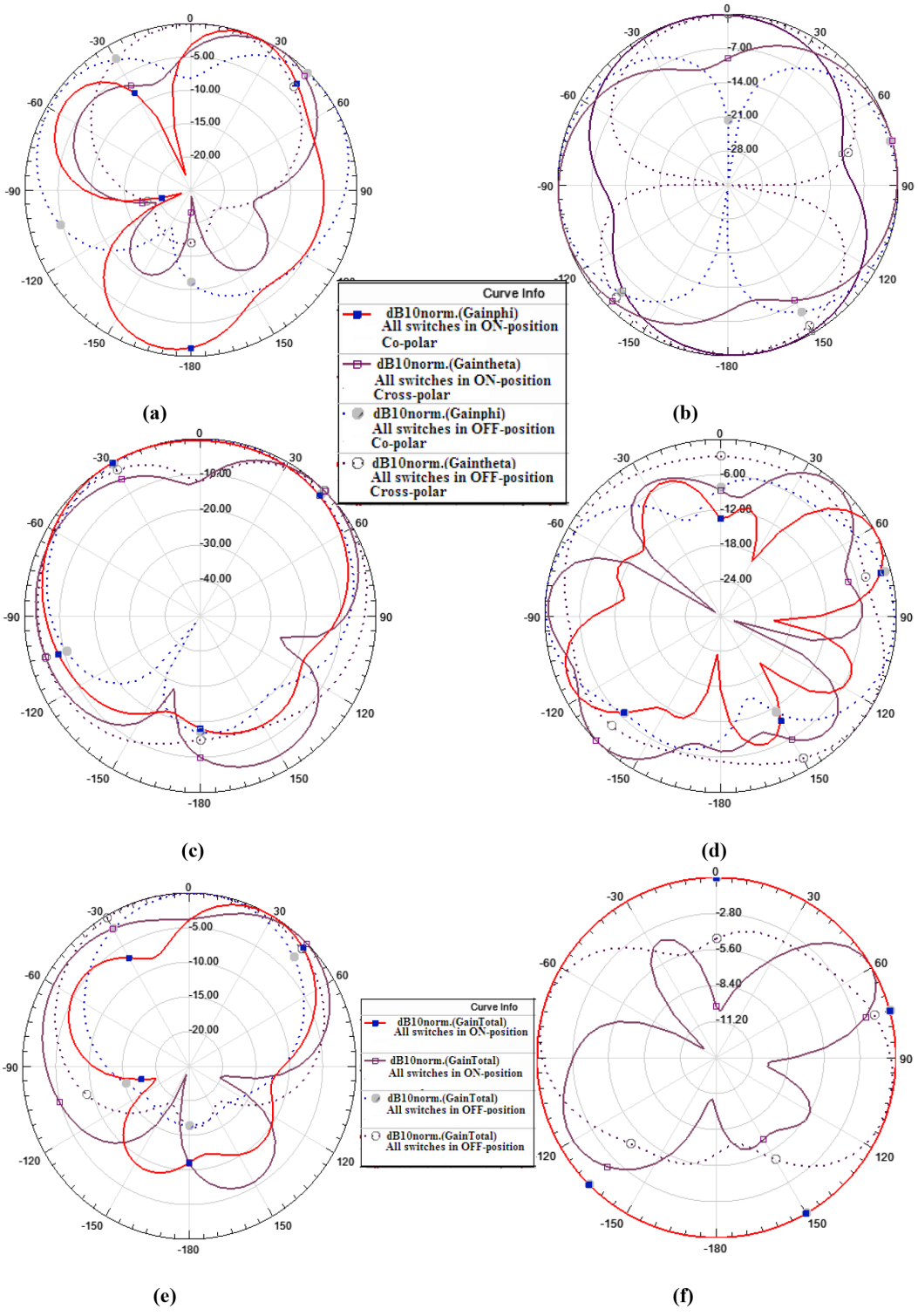

Figure 10. Normalized co-, cross-polar, and total gain radiation patterns in E-plane and H-plane for the RA at extreme switching configurations: (a) XZ-plane ($\emptyset = 0$), (b) XY-plane ($\theta = 0$), (c)YZ-plane ($\emptyset = 90$), (d) gainphi and gaintheta ($\theta = 90$), (e) gain total ($\emptyset = 0$, $\emptyset = 90$), (f) gain total ($\theta = 0$, $\theta = 90$).

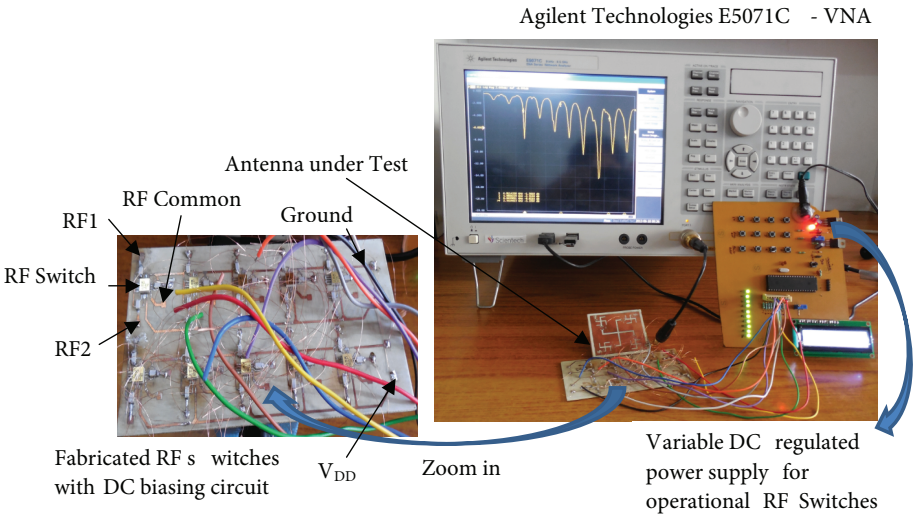

Figure 11. Reconfigurable swastika-antenna measurement setup for return loss characterization.

Table 5. Comparison of simulated and measured S-parameter of proposed antennas with and without RF switches.

Antenna configuration (Switching/nonswitching state)	Resonating freq. (GHz)		RL (S_{11}) in dB		Bandwidth (MHz)		Applications of proposed antennas
	Simulated	Measured	Simulated	Measured	Simulated	Measured	Typical uses
Swastika fractal antenna for 0th iteration	2.32 2.58 6.44	2.41 2.52 6.38	−16.65 −12.09 −10.59	−14.32 −11.97 −11.08	122.60 44.80 108.9	118.40 46.34 106.36	Bluetooth/UMTS 4GWiMAX/IEEE 802.16 Personal communication
Swastika fractal antenna for 1st iteration	2.11 2.98 4.08 6.02	2.10 3.02 4.03 6.11	−28.79 −10.36 −11.37 −31.68	−26.46 −11.24 −11.02 −29.12	185.8 22.34 24.14 293.1	178.68 24.56 26.32 288.64	GSM/CDMA 4GWiMAX/IEEE 802.16 Personal communication Personal communication
Swastika fractal antenna for 2nd iteration (without switches)	2.14 2.86 3.93 4.15 5.89	2.12 2.96 3.98 4.08 5.81	−22.51 −12.09 −12.35 −14.62 −26.02	−20.54 −11.98 −11.85 −14.20 −24.86	174.6 30.54 32.12 46.26 531.8	172.42 28.86 34.86 48.84 526.64	GSM/CDMA 4GWiMAX/IEEE802.16 Personal communication Personal communication WLAN/IEEE 802.11a
Reconfigurable swastika fractal antenna for 2nd iteration (all switches in on position)	2.40 2.52 4.33 5.37 6.27	2.40 2.53 4.29 5.40 6.31	−17.69 −19.76 −12.43 −10.16 −20.90	−16.97 −18.14 −11.33 −10.88 −19.87	64.10 80.10 52.10 22.18 258.28	66.42 82.26 54.68 28.42 252.46	Bluetooth/UMTS/Wi-Fi 4G/LTE Personal communication WirelessLAN/IEEE802.11a Personal communication
Reconfigurable swastika fractal antenna for 2nd iteration (all switches in	2.35 2.59 4.37	2.31 2.52 4.29	−18.56 −20.04 −12.71	−16.77 −18.84 −12.45	66.10 90.10 54.10	68.48 92.72 56.28	Wi-Fi /IEEE802.11 4G/LTE Personal communication

switches was designed, fabricated, and tested. For all possible RF switching states, the results of the proposed reconfigurable antenna worked well for frequencies lying between 1.5 and 7.5 GHz. From an industrial application point of view, the proposed compact reconfigurable antenna is considered in the mobile RF front end terminal, which covers the maximum present as well as future wireless and mobile communication bands like UMTS (IMT-2000), 4G WiMAX/IEEE 802.16, and WLAN (5.8 GHz)/IEEE 802.11a (outdoor) wireless communications, while at the same time retaining a sensible integrity in its reasonable bandwidth characteristics.

Acknowledgments

This work was supported by the National Program on Micro and Smart Systems (NPMASS) and also MANCEF, New Mexico, USA, along with the Coventor organization, providing Coventorware, Comsol, and other useful software.

References

[1] Werner DH, Gangul S. An overview of fractal antenna engineering research. IEEE Antenn Propag M 2003; 45: 38–57.

[2] Werner DH, Haup RL, Werner PL. Fractal antenna engineering: the theory and design of fractal antenna arrays. IEEE Antenn Propag M 1999; 41: 37–58.

[3] Puente C, Romeu J, Pous R, Garcia X, Benitez F. Fractal multiband antenna based on the Sierpinski gasket. Electron Lett 1996; 32: 1–2.

[4] Tang PW, Wahid PF. Hexagonal fractal multiband antenna. IEEE Antenn Wirel Pr 2004; 3: 111–112.

[5] Chawla P, Khanna R. Optimization algorithm of neural network on RF MEMS switch for wireless and mobile reconfigurable antenna applications. In: Second IEEE International Conference on PDGC-2012; 6–8 December 2012; Solan, India. New York, NY, USA: IEEE. pp. 735–740.

[6] Chawla P, Khanna R. A novel design and optimization approach of RF MEMS switch for reconfigurable antenna using ANN method. In: IEEE Conference on Communications, Devices and Intelligent Systems; 28–29 December 2012; Kolkata, India. New York, NY, USA: IEEE. pp. 188–191.

[7] Singh J, Singh AP, Kamal TS. Design of circular microstrip antenna using artificial neural networks. In: Proceedings of World Congress on Engineering 2011, Vol. 2; 6–8 July 2011; London, UK. pp. 1013–1016.

[8] Türker N, Güneş F, Yıldırım T. Artificial neural design of microstrip antennas. Turk J Electr Eng Co 2006; 14: 445–453.

[9] Chawla P, Khanna R. Multiband fractal based reconfigurable antenna with introduction of RF MEMS switches for next generation devices. Int J Phys Sci 2013; 8: 1628–1638.

[10] Anagnostou DE, Zheng G, Chryssomallis MT, Lyke JC, Ponchak GE, Papapolymerou J, Christodoulou CG. Design, fabrication, and measurements of an RF-MEMS-based self-similar reconfigurable antenna. IEEE T Antenn Propag 2006; 54: 422–432.

[11] Garg A, Chawla P, Khanna R. A novel approach of RF MEMS resistive series switch for reconfigurable antenna. In: Proceedings of IEEE International Conference on Microelectronics, Communication & Renewable Energy; 4–6 June 2013; Kerala, India. New York, NY, USA: IEEE. pp. 1–6.

[12] Sevinç Y, Kaya A. Reconfigurable antenna structure for RFID system applications using varactor-loading technique. Turk J Electr Eng Co 2012; 20: 453–462.